Vol. 6, No. 4, 2015
ISSN 2233-4203/ e-ISSN 2093-8950
LETTER www.msletters.org | Mass Spectrometry Letters

Applications of Stochastic Process in the Quadrupole Ion traps

Sarkhosh Seddighi Chaharborj,[1,2,3]* Seyyed Mahmod Sadat Kiai,[3] Norihan Md Arifina,[1] and Yousof Gheisari[2]

[1]Department of Mathematics,Faculty of Science,Universiti Putra Malaysia,43400 UPM, Malaysia
[2]Department of Mathematics, Science and Research Branch, Islamic Azad University, Bushehr Branch, Bushehr, Iran
[3]Plasma Physics and Nuclear Fusion Research school, Nuclear Science and Technology Research Institute (NSTRI), P.O. Box 14395-836, Tehran, Iran

Received December 28, 2014; Revised March 20, 2015; Accepted May 29, 2015
First published on the web December 31, 2015; DOI: 10.5478/MSL.2015.6.4.91

Abstract : The Brownian motion or Wiener process, as the physical model of the stochastic procedure, is observed as an indexed collection random variables. Stochastic procedure are quite influential on the confinement potential fluctuation in the quadrupole ion trap (QIT). Such effect is investigated for a high fractional mass resolution $\Delta m/m$ spectrometry. A stochastic procedure like the Wiener or Brownian processes are potentially used in quadrupole ion traps (QIT). Issue examined are the stability diagrams for noise coefficient, $\eta = 0.07;0.14;0.28$ as well as ion trajectories in real time for noise coefficient, $\eta = 0.14$. The simulated results have been obtained with a high precision for the resolution of trapped ions. Furthermore, in the lower mass range, the impulse voltage including the stochastic potential can be considered quite suitable for the quadrupole ion trap with a higher mass resolution.

Keywords : Stochastic process, Quadrupole ion trap, Ion motion, Fractional mass resolution.

Introduction

There is the possibility that an ion trap mass spectrometer incorporates such traps as the Penning,[1] Paul[2] or Kingdon[3] traps. In 2005, the Orbitrap was introduced according to the Kingdon trap.[4] The two most popular kinds of ion traps are the Penning and the Paul traps (quadrupole ion trap).[5-8] Of course, it is also possible that other kinds of mass spectrometers utilize a linear quadrupole ion trap selected as a mass filter. Interestingly, ion trap mass spectrometry has undergone many developmental stages in order to achieve its current condition with relatively high performance level and growing popularity. Paul and Steinwedel[9] invented Quadrupole ion trap (QIT) commonly used in mass spectrometry,[5-8] ion cooling and spectroscopy,[10] frequency standards,[11] quantum computing[12] and others. However, different geometries have also been suggested and utilized for QIT.[13]

*Reprint requests to Sarkhosh Seddighi Chaharborj
E-mail: sseddighi2007@yahoo.com

Main properties of Wiener process

A Wiener process[14,15] (notation $W = (W_t)_{t\geq 0}$) is named in the honor of Prof. Norbert Wiener; other name is the Brownian motion (notation $B = (B_t)_{t\geq 0}$). Wiener process is Gaussian process. As any Gaussian process, Wiener process is completely described by its expectation and correlation functions[14,15]

Main properties of $W = (W_t)_{t\geq 0}$:

- $W_0 = 0$
- Trajectories of Wiener process are continues functions of $t \in [0,\infty]$ (see Figure (1)),
- expectation $E[W_t] = 0$,
- correlation function $E[W_t W_s] = \min(t,s)$,
- for any $t_1, t_2, ..., t_n$ the random vector $(W_{t_1}, W_{t_2}, ..., W_{t_n})$ is Gaussian,
- for any s,t
  $E[W_t^2] = t$
  $E[W_t - W_s] = 0$
  $E[W_t - W_s]^2 = |t-s|$
- Increments of Wiener process on non overlapping intervals are independent, i.e. for $(s_1,t_1)\cap(s_2,t_2) = 0$ the random variables $W_{t_2} - W_{s_2}$, $W_{t_1} - W_{s_1}$ are independent,
- paths of Wiener process are not differentiable functions,
- martingale property,
  $E[W_t | W_0^s] = W_s$
  $E[(W_t - W_s)^2 | W_s] = t - s$
- here $W_0^s = \{W_u | 0 \leq u \leq s\}$.

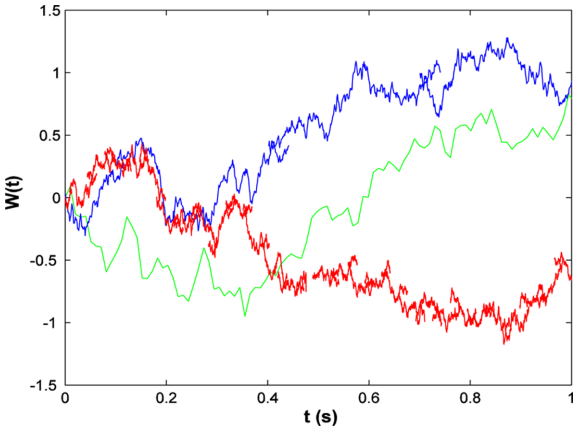

Figure 1. Realization of W_t^N for N = 100 (green), N = 1000 (blue) and N = 10000 (red).

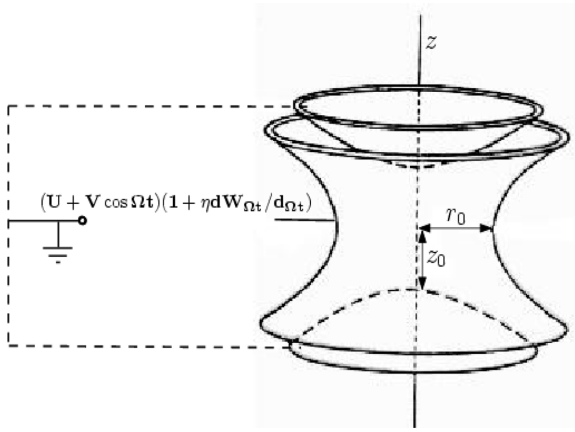

Figure 2. This figure show a schematic view of a quadrupole ion trap.

Wiener process as a scald random walk

Consider a simple random walk $X_{n\in N}$ on the lattice of integers Z,

$$X_n = \sum_{k=1}^{n} \xi_k ,$$

where $\{\xi_k\}_{k\in N}$ is a collection of independent, identically distributed random variables with $P(\xi_k = \pm 1) = 1/2$. From the Central Limit Theorem[16,17] we have,

$$\frac{X_n}{\sqrt{N}} \to N(0,1) ,$$

in distribution as $N \to \infty$. Here $N(0,1)$ is the Gaussian variable with mean 0 and variance 1. This suggests to define the piecewise constant random function W_t^N on $t \in [0,\infty]$ by letting,

$$W_t^N = X_{\lfloor Nt \rfloor}/\sqrt{N} , \ (\lfloor . \rfloor \text{ is floor function})$$

In can be shown that as $N \to \infty$, W_t^N converges in distribution to a stochastic process W_t, termed the Wiener process or Brownian motion.[14-17]

The motions of ion inside quadrupole ion trap with stochastic potential form

Fig. (2) shows indicatesa the schematic perspectives of a quadrupole ion trap (QIT). The quadrupole ion trap is the ion trap which including hyperbolic geometry and also is composed of involves a ring and two end cap electrodes that facing face each other in the z-axis (see Fig. (2)). Here, z_0 can also be considered the distance that begins started from the center of the QIT to the end cap. Also, r_0 is regarded as the distance from the outset point in the center of the QIT and extends to the nearest ring surface. Forcing the particles to swing and vibrate in confined space[6,18-20] can be the best approach for trapping charged particles. Such force can be written as follows,

$$K = -kR \tag{1}$$

Where R is regarded as the distance from the center of the swing to the particle position and k is seen as a constant. Such force generated via the parabolic potential will move the oscillating particle around the equilibrium point. It can be expressed as follows,

$$\Phi = -\int F.dR = \frac{1}{2}kR^2 = \frac{1}{2}k(r^2 + z^2) \tag{2}$$

Here, $R^2 = r^2 + z^2$, $r^2 = x^2 + y^2$. Also, x, y, z can be considered as Cartesian space components. Furthermore, any possible free space should satisfy the Laplace equation, given as follows,

$$\nabla^2 \Phi = 0 \tag{3}$$

As Eq. (2) is unable to satisfy the Laplace situation, thus for confining the ions in two dimensions, it seems to be necessary to use a complicated potential as follows,

$$\Phi(x,y,z) = A(\alpha x^2 + \beta y^2 + \gamma z^2) \tag{4}$$

For satisfying Eq. (4), in a Laplace situation, $\nabla^2 \Phi = 0$, the following equations are required, $\alpha = \beta = 1$, $\gamma = -2$. Therefore,

$$\Phi(x,y,z) = A(x^2 + y^2 - 2z^2) = A(r^2 - 2z^2) \tag{5}$$

This possibility is generated via four hyperbolic electrodes. In order to achieve such type of electrodes, the surfaces can be considered with the same potential $\Phi_0/2$ and $-\Phi_0/2$, as follow,

$$\Phi(r_0, 0) = \Phi_0/2 \ \text{ and } \ \Phi(0, z_0) = -\Phi_0/2 . \tag{6}$$

These situations make us able to find, $A = \Phi_0/2r_0^2$ and

$A = \Phi_0/4z_0^2$, therefore $r_0^2 = 2z_0^2$. Consequently, electrodes shaped for the potential (4) can be obtained as follows,

$$\Phi = \frac{\Phi}{2r_0^2}(r^2 - 2z^2) = \pm 1 \tag{7}$$

Eq. (7) represeznts a hyperbolic equation for this potential. Also, the potential Φ_0 used in hyperbolic electrodes is as follow,

$$\Phi_0 = (U - V\cos(\Omega t)) \tag{8}$$

thus, the stochastic potential, $(\Phi_0)_{st}$, can be written as,

$$\begin{aligned}(\Phi_0)_{st} &= \Phi_0 + \text{random part},\\ &= \Phi_0 + \Phi_0(\eta dW_{\Omega t}/d_{\Omega t})\end{aligned} \tag{9}$$

where W_t is a Wiener procedure and $\eta > 0$ is the noise coefficient determining the size of the stochastic term.[14,15] In this regard, the noise coefficient, η, explains the amount of fluctuation potentially. For $\eta = 0$, the deterministic potential or normal potential can be stated as $(\Phi_0)_{st} = \Phi_0$. Here, the parameter is selected, therefore $\sqrt{\text{Varinace}[\cos(\Omega t)]}$ is set to be about 14% as a common fluctuation in a potential. Also, the potential Φ_{st} is usually written as follows,

$$\Phi_{st} = \frac{1}{2r_0^2}(r^2 - 2z^2)(\Phi_0)_{st} \tag{10}$$

field elements in the trap therefore becomes,

$$(E_r, E_z) = -\nabla\Phi(r, z) \tag{11}$$

Where ∇ is the gradient. From Eq. (11) we obtain,

$$(E_r, E_z) = \begin{bmatrix} -\frac{r}{r_0^2}(\Phi_0)_{st} \\ \frac{2z}{r_0^2}(\Phi_0)_{st} \end{bmatrix} \tag{12}$$

The equations of motion for a singly charged positive ion in the QIT is represented thusly,

$$\begin{aligned}\frac{d^2z}{d\xi^2} + (a_z - 2q_z\cos 2\xi)(1 + \eta dW_\xi/d\xi)z = 0\\ \frac{d^2r}{d\xi^2} + (a_r - 2q_r\cos 2\xi)(1 + \eta dW_\xi/d\xi)r = 0\end{aligned} \tag{13}$$

The a and q are for the z and r parts and the dimensionless parameter ξ are as follows,

$$\xi = \frac{\Omega t}{2},\ a_z = -2a_r = \frac{4eU}{mz_0^2\Omega^2},\ q_z = -2q_r = \frac{2eV}{mz_0^2\Omega^2}, \tag{14}$$

where m can be regarded as the ion mass and e as the electronic charge.

Thus, $\Omega/2\pi$ is considered as the drive radio frequency (rf), z_0 as one-half the shortest separation of the end cap electrodes, $r_0 = 2z_0^2$ as the square of ring electrode radius and a_z and q_z as the trapping parameters. The standard Wiener procedure can be defined by a time step $d\xi$ as follows,

$$\frac{dW_\xi}{d\xi} \sim \frac{\sqrt{d\xi}}{d\xi}N(0, 1) \tag{15}$$

here, $N(0, 1)$ is seen as the standard normal distribution that is the normal distribution including mean $\mu = 0$ and variance $\sigma^2 = 1$ and density function given as,

$$\phi(z) = \frac{1}{\sqrt{2\pi}}e^{-\frac{1}{2}z^2} \tag{16}$$

In Matlab, the command "randn" was used to add the elements of distribution $N(0, 1)$.

Fig. (3) compares the periodic impulsional potential of the form $\eta\cos(\Omega t)dW_{\Omega t}/d_{\Omega t}$, for $\eta = 0.0;0.7;0.14;0.28$.

Numerical results

Stability regions

Two stability parameters monitor the ion motion for each dimension z ($z = z$ or $z = r$) and a_z, q_z in the cases of the quadrupole ion trap for deterministic and stochastic cases respectively. The ion's stable and unstable motions, in the plane (a_z, q_z) and for the z axis, can be determined through making comparison between the amplitude of the movement and different values of a_z, q_z. For calculating the precise elements of the motion equations for the stability diagrams, a numerical approach was used. The fifth order Runge-Kutta approach (using 0.001 stepwise increments) was used via the Matlab software as well as the scanning approach.

Fig. (4) displays the calculated first stability area for the quadrupole ion traps including and excluding the stochastic potential, red points (red color): QIT, blue circles (blue color): stochastic QIT, (a): $\eta = 0.07$, (b): $\eta = 0.14$ and (c): $\eta = 0.28$. Fig. (4) indicates that increasing noise coefficient η, decreases the first stability area.

Ion trajectories

Fig. (5) indicates the ion trajectories in real time for stochastic as well as deterministic cases including $a_z = -2a_r = 0$ and $q = -2q_r = 0.4$. Indications are done by a solid line (green line): $\xi - z$ for deterministic case, dash line (black line): $\xi - z_{st}$ for stochastic case when $\eta = 0.14$. Here "st" stands for "stochastic".

From a mathematical viewpoint, stochastic as well as theoretical results are closely related. Thus, employing stochastic procedure in quadrupol ion trap potential makes us able to simulate and obtain the numerical outcomes including high accuracy (see Figs. (5)). Table (1) reveals the

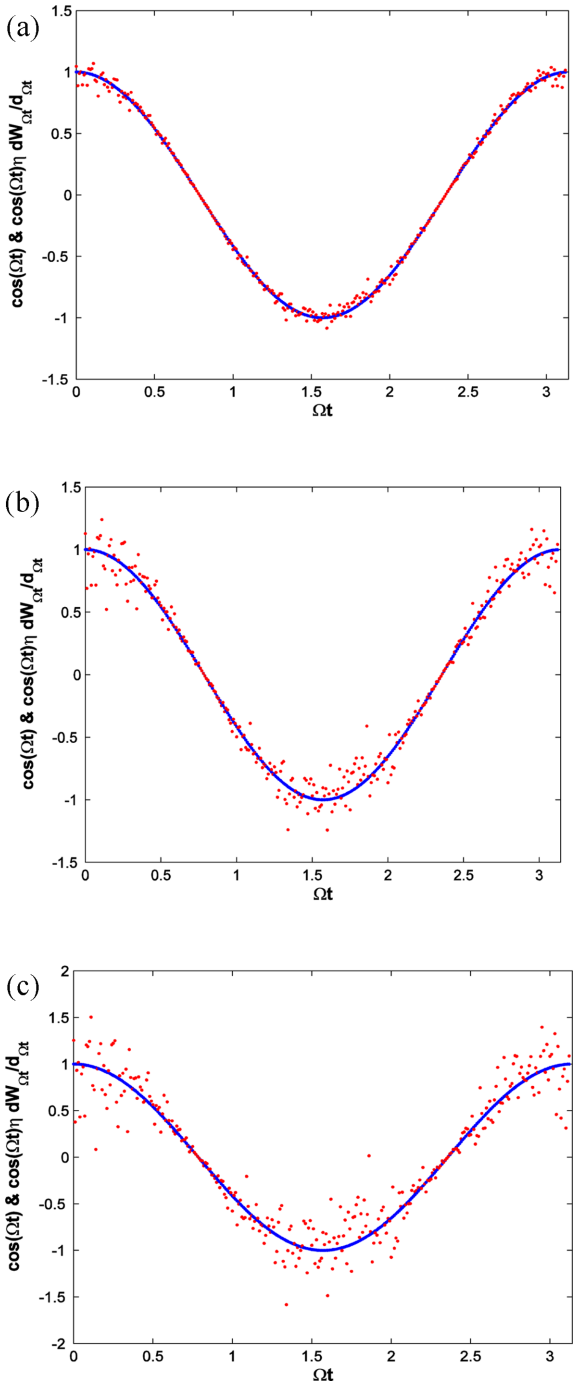

Figure 3. Shape of potential function for the impulsional potentials of the form $\eta\cos(\Omega t)dW_{\Omega t}/d_{\Omega t}$; blue color: $\eta = 0$ and red color: $\eta = 0.07;0.14;0.28$ for (a), (b) and (c), respectively.

values of q_z for QIT including and excluding the stochastic potentials for the equivalent points. Thus, two operating points observed in their corresponding stability diagram have the same β_z: $\beta_z = 0.3;0.6;0.9$. For the computations, the following equations can be used,

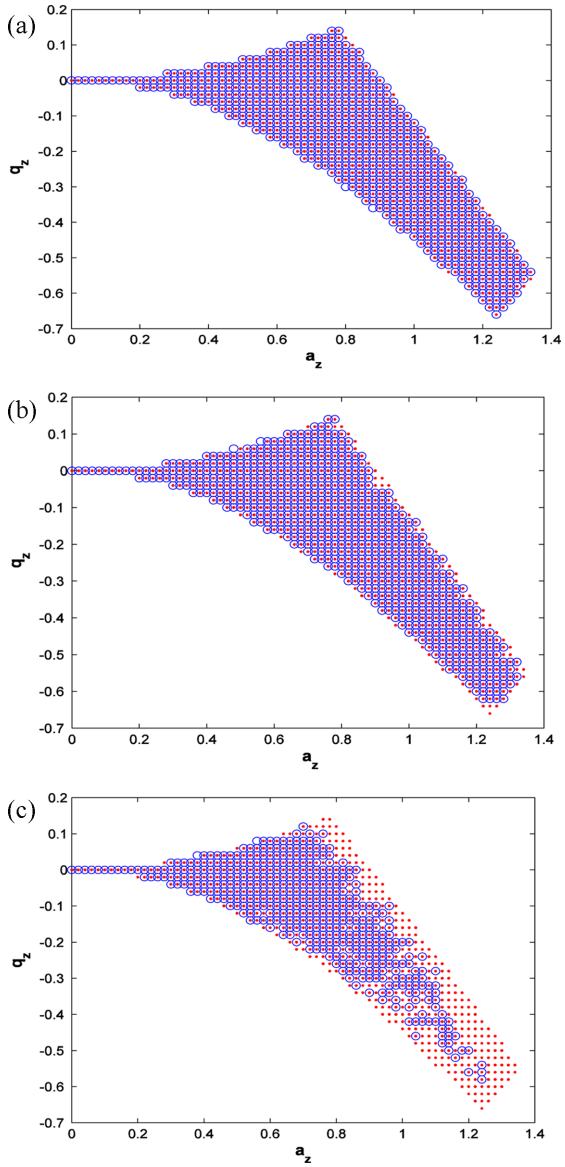

Figure 4. The first stability regions, red points: QIT, blue circles: stochastic QIT, (a): $\eta = 0.07$, (b): $\eta = 0.14$ and (c): $\eta = 0.28$; with initial conditions, $z(0) = 0.01$, $\dot{z}(0) = 0$, $r(0) = 0.01$ and $\dot{r}(0) = 0$.

$$\frac{a_z-\beta^2}{q_z} = \cfrac{1}{\frac{a_z-\beta^2}{q_z} - \cfrac{1}{\frac{a_z-(2+\beta)^2}{q_z} - \cfrac{1}{\frac{a_z-(4+\beta)^2}{q_z} - \ldots}}} + \cfrac{1}{\frac{a_z-\beta^2}{q_z} - \cfrac{1}{\frac{a_z-(\beta-2)^2}{q_z} - \cfrac{1}{\frac{a_z-(\beta-4)^2}{q_z} - \ldots}}}$$

and (17)

$$\frac{a_z-\beta^2}{q_z\left(1+\eta\dfrac{\overline{dW_\xi}}{d\xi}\right)}=\cfrac{1}{\dfrac{a_z-\beta^2}{q_z\left(1+\eta\dfrac{\overline{dW_\xi}}{d\xi}\right)}-\cfrac{1}{\dfrac{a_z-(2+\beta)^2}{q_z\left(1+\eta\dfrac{\overline{dW_\xi}}{d\xi}\right)}-\cfrac{1}{\dfrac{a_z-(4+\beta)^2}{q_z\left(1+\eta\dfrac{\overline{dW_\xi}}{d\xi}\right)}-\ldots}}}+\cfrac{1}{\dfrac{a_z-\beta^2}{q_z\left(1+\eta\dfrac{\overline{dW_\xi}}{d\xi}\right)}-\cfrac{1}{\dfrac{a_z-(\beta-2)^2}{q_z\left(1+\eta\dfrac{\overline{dW_\xi}}{d\xi}\right)}-\cfrac{1}{\dfrac{a_z-(\beta-4)^2}{q_z\left(1+\eta\dfrac{\overline{dW_\xi}}{d\xi}\right)}-\ldots}}}$$

Here $\overline{dW_\xi}/d\xi$ is the mean of $dW_\xi/d\xi$.

Table (1) indicates the values of q_z for the quadrupole ion trap including and excluding the stochastic potential with $\eta = 0.07;0.14;0.28$ and $\beta_z = 0.3;0.6;0.9$ when $a_z = 0$. From Table (1) we see that an increase in the parameter η, will decrease q_z for different values of β.

The values of $q_{z_{max}}$ when $a_z = 0$ for the quadrupole ion trap with and without stochastic potential in the first stability region when $\eta = 0.07;0.14;0.28$ is presented in Table (2).

Table (3) represents the values of $V_{z_{max}}$ as $a_z = 0$ for ^{131}Xe with $\Omega = 2\Pi\times1.05\times10^6$ rad/s, $U = 0$ V, $z_0 = 0.783$ cm in the first stability area when $\eta = 0.07;0.14;0.28$. Table (3) reveals that as η increases, $V_{z_{max}}$ will increase too. To obtain the values of Table (3) by using Eq. (15) we presume $V_{z_{max}}$ is the function of m, z_0, Ω^2, e and $1+\eta(\overline{dW_\xi}/d\xi)$ is written as follows,

$$V_{z_{max}} \propto \frac{mz_0^2\Omega^2\left(1+\eta\dfrac{\overline{dW_\xi}}{d\xi}\right)}{2e} \quad (18)$$

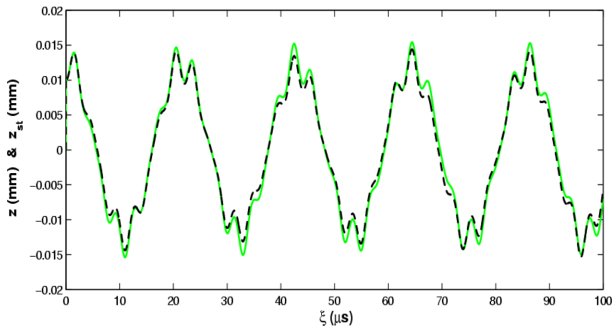

Figure 5. The ion trajectories in real time with $a_z = -2a_r = 0$ and $q_z = -2q_r = 0.4$, solid line (green line): $\xi - z$ for deterministic case, dash line (black line): $\xi - z_{st}$ for stochastic case when $\eta = 0.14$; with initial conditions, $z(0) = 0.01$ and $\dot{z}(0) = 0$.

Now, we use Eq. (19) to calculate $V_{z_{max}}$ for ^{131}Xe with $\Omega = 2\Pi\times1.05\times10^6$ rad/s and $z_0 = 0.783$ cm when $\eta = 0;0.14$ as follows,

$$V_{z_{max}} = \frac{(131/(6.022\times10^{26}))\times(0.783\times10^{-2})^2}{2\times1.602\times10^{-19}} \times(2\pi\times1.05\times10^6)^2\times(1+0)\approx5455$$

$$V_{z_{max}} = \frac{(131/(6.022\times10^{26}))\times(0.783\times10^{-2})^2}{2\times1.602\times10^{-19}} (2\pi\times1.05\times10^6)^2\times(1+0.014)\approx6983$$

Fig. (6A) shows the behavior of function $q_z(\eta)$ for $\beta_z = 0.3;0.6;09$ when $a_z = 0$. As β_z increase, the difference $q_z(0.07)-q_z(0.28)$ will also increase.

Fig. (6B) shows $q_{z_{max}}$ and $V_{z_{max}}$ as a function of η in a QIT determined for the first stability area as $0\le\eta<0.28$ in parts (a) and (b), respectively. To plot Fig. (6B), we have to used Table and Table when $\eta = 0;0.07;0.14;0.28$. Fig. (6B.a) shows that when all factors increase, there is an outcome decrease and Fig. (6B.b) shows that with increasing parameter η; the values of $q_{z_{max}}$ increases also. Higher V_{rf} is shown to have better mass separation particularly for the lower ion mass range.

The effect of stochastic potential form on the mass resolution

Generally, the resolution of a quadrupole ion trap mass spectrometry[21] can be regarded as a function of the mechanical precision of the hyperboloid of the QIT Δr_0, and the stability performances of electronics tools like, variations in voltage amplitude ΔV and the rf frequency $\Delta\Omega$ [21] which tells us how precise the type of voltage signal

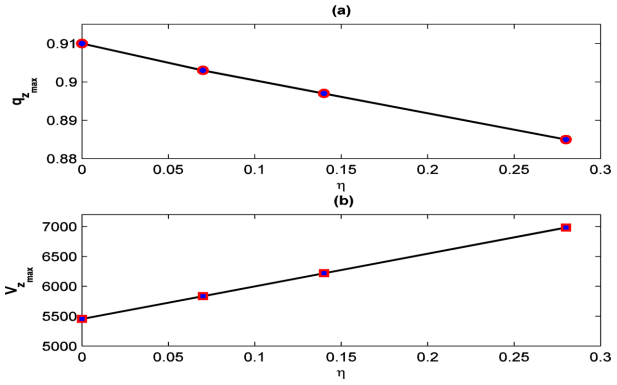

Figure 6. (A): The behavior of function $q_z(\eta)$ for $\beta_z = 0.3;0.6;0.9$ when $a_z = 0$, (B): The behavior of $q_{z_{max}}(\eta)$ and $V_{z_{max}}(\eta)$ in the first stability region when $a_z = 0$, (a): $q_{z_{max}}(\eta)$ and (b): $V_{z_{max}}(\eta)$ for ^{131}Xe with $\Omega = 2\pi\times1.05\times10^6$ rad/s, $U = 0$ V, $z_0 = 0.783$ cm.

used. The present study considers the resolution of a quadrupole ion trap including and excluding stochastic potential. The factor $\eta(\overline{dW_\xi/d\xi})$ is very significant in plotting stability diagrams and potential for the goal of the mass resolution.

For deriving an influential theoretical formula for fractional resolution, we should consider the stability parameters of the impulse excitation for the QIT including and excluding its stochastic potential, respectively as follows,

$$q_z = 4\frac{e}{m}\times\frac{V}{r_0^2\Omega^2} \tag{19}$$

$$q_{z_{st}} = 4\frac{e}{m}\times\frac{V_{st}\left(1+\eta\overline{\frac{dW_\xi}{d\xi}}\right)}{r_0^2\Omega^2} \tag{20}$$

By taking the partial derivatives associated with the variables of the stability parameters q_z for Eq. (20) and $q_{z_{st}}$ for Eq. (21), the expression of the resolution Δm of the QIT including and excluding stochastic potential are as follows,

$$\Delta m = \left(\frac{8eV}{r_0^3\Omega^2 q_z}\right)|\Delta r_0| + \left(\frac{4e}{r_0^2\Omega^2 q_z}\right)|\Delta V| + \left(\frac{8eV}{r_0^2\Omega^3 q_z}\right)|\Delta\Omega| \tag{21}$$

$$\begin{aligned}(\Delta m)_{st} = &\left(\frac{8eV_{st}\left(1+\eta\overline{\frac{dW_\xi}{d\xi}}\right)}{r_0^3\Omega^2 q_{z_{st}}}\right)|\Delta r_0| + \left(\frac{4e\left(1+\eta\overline{\frac{dW_\xi}{d\xi}}\right)}{r_0^2\Omega^2 q_{z_{st}}}\right)|\Delta V_{st}| \\ &+\left(\frac{8eV_{st}\left(1+\eta\overline{\frac{dW_\xi}{d\xi}}\right)}{r_0^2\Omega^3 q_{z_{st}}}\right)|\Delta\Omega| + \left(\frac{4eV_{st}}{r_0^2\Omega^2 q_{z_{st}}}\right)\left|\Delta\left(\eta\overline{\frac{dW_\xi}{d\xi}}\right)\right|\end{aligned} \tag{22}$$

Now, in order to find the fractional resolution, we have,

$$\frac{m}{\Delta m} = \left\{\left|\frac{\Delta V}{V}\right| + 2\left|\frac{\Delta\Omega}{\Omega}\right| + 2\left|\frac{\Delta r_0}{r_0}\right|\right\}^{-1} \tag{23}$$

$$\left(\frac{m}{\Delta m}\right)_{st} = \left\{\left|\frac{\Delta V_{st}}{V_{st}}\right| + 2\left|\frac{\Delta\Omega}{\Omega}\right| + 2\left|\frac{\Delta r_0}{r_0}\right| + \frac{\Delta\left(\eta\overline{\frac{dW_\xi}{d\xi}}\right)}{1+\eta\overline{\frac{dW_\xi}{d\xi}}}\right\}^{-1} \tag{24}$$

here Eq. (24) and Eq. (25) are the fractional resolutions for QIT with and without stochastic potential, respectively.

Fig. (7a) indicates the fractional resolution that is a function of the noise coefficient η and Fig. (7b) displays the resolution of Δm that is a function of ion mass m, where a

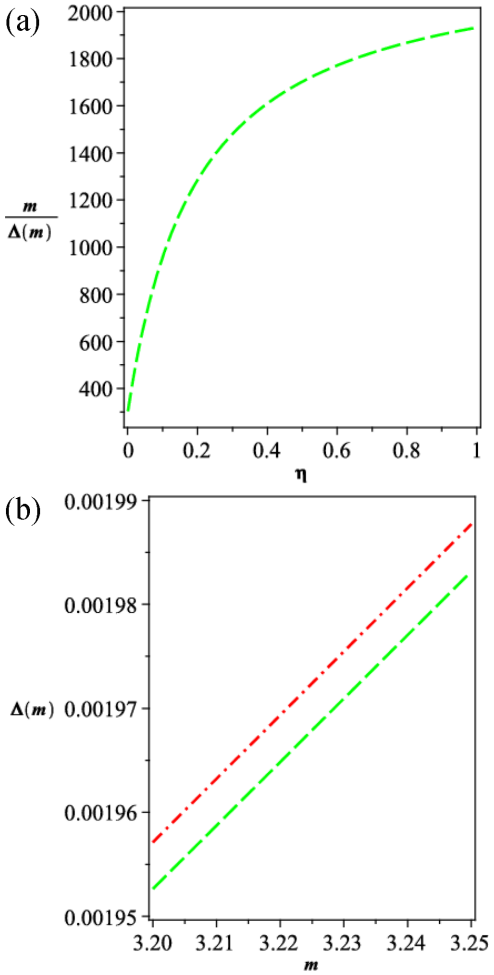

Figure 7. The fractional resolution as a function of the noise coefficient η, (b) resolution of Δm as function of ion mass m, dash dot line (red line): deterministic case ($\eta = 0$) and dash line (green line): stochastic case ($\eta = 0.14$).

dash dot line (red line); represents deterministic cases ($\eta = 0$) and dash lines (green line) represent stochastic case ($\eta = 0.14$).

Regarding the fractional mass resolution, the following uncertainties were used for the voltage, rf frequency and the geometry; $\Delta V/V = 10^{-5}$, $\Delta\Omega/\Omega = 10^{-7}$, $\Delta r_0/r_0 = 3\times10^{-4}$, for $\eta = 0;0.07;0.14;0.28$ we have assumed arbitrarily the the noise coefficient $\Delta\eta = 10^{-2}$. The fractional resolutions obtained are $(m/\Delta m)_{st} = 298;812;1113;1448$ for $\eta = 0;$ 0.07;0.14;0.28, respectively. When stochastic potential is applied ($\eta = 0.14$), the limited voltage of rf increases by a factor of approximately 1.14; thus, the voltage uncertainties were taken as $\Delta V_{st}/V_{st} = 1.14\times10^{-5}$. Once these fractional resolutions were considered for the tritium isotope mass $m = 3.202348$, then, $\Delta m = 0.001954$ and 0.001959 with and without stochastic potential, the values for $\eta = 0$ and $\eta = 0.14$ were achieved, respectively.

Theoretically, we have,

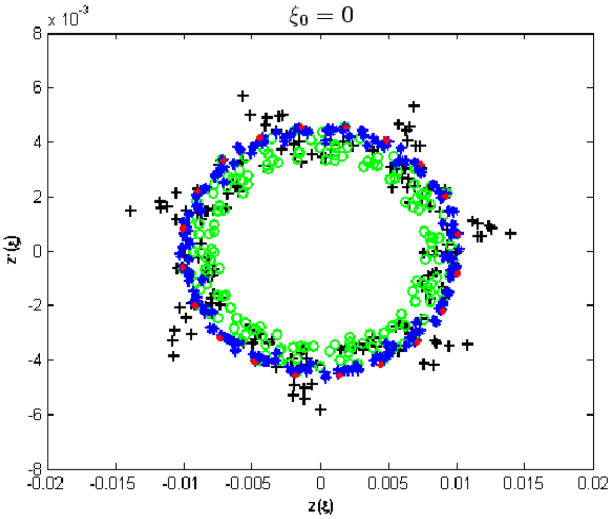

Figure 8. The evolution of the phase space ion trajectory for different values of the phase $\xi_0 = 0$ for $\beta_z = 0.3$, red line: $\eta = 0$ ($q_z = 0.40944$), blue line: $\eta = 0.07$ ($q_z = 0.40659$), green line: $\eta = 0.14$ ($q_z = 0.40379$) and black line: $\eta = 0.28$ ($q_z = 0.39829$).

$$\frac{\Delta m}{m} = \left|\frac{\Delta V}{V}\right| + 2\left|\frac{\Delta\Omega}{\Omega}\right| + 2\left|\frac{\Delta r_0}{r_0}\right| \le \left|\frac{\Delta V_{st}}{V_{st}}\right| + 2\left|\frac{\Delta\Omega}{\Omega}\right| + 2\left|\frac{\Delta r_0}{r_0}\right|$$

$$\le \left|\frac{\Delta V_{st}}{V_{st}}\right| + 2\left|\frac{\Delta\Omega}{\Omega}\right| + 2\left|\frac{\Delta r_0}{r_0}\right| + \left|\frac{\Delta\left(\eta\overline{\frac{dW_\xi}{d\xi}}\right)}{1+\eta\overline{\frac{dW_\xi}{d\xi}}}\right| = \left(\frac{\Delta m}{m}\right)_{st}$$

Thus, $(m/\Delta m)_{st} \ge m/\Delta m$. This means that, along with increasing η the value of $m/\Delta m$ will increase. Therefore, the power of resolution will increase because of the reduction in Δm. Experimentally, this means that the width of the mass signal spectra is better separated.

Phase space ion trajectory

Fig. (8) indicates the evolution of the phase space ion trajectory for different values of the phase $\xi_0 = 0$ for $\beta_z = 0.3$ where by a red line indicates $\eta = 0$ ($q_z = 0.40944$), a blue line a blue line indicates $\eta = 0.07$ ($q_z = 0.40659$), a green line indicates $\eta = 0.14$ ($q_z = 0.40379$) and a black line for $\eta = 0.28$ ($q_z = 0.39829$).

The results represented in Fig. (8) indicates that for the same equivalent operating point in the two stability diagrams (having the same $\beta_z = 0.3$), the associated modulated secular ion frequencies behavior is almost the same for different values of $\eta = 0;0.07;0.14;0.28$.

Discussion and conclusion

From a mathematical point of view, the results of stochastic process has higher resolution during mass separation. It has been shown that $(m/\Delta m)_{st} \ge m/\Delta m$, this means that, with increase in η the value of $m/\Delta m$ also increases and therefore the power of resolution increases too due to a reduction in Δm. Empirically, the width of the mass signal spectra seems to be better separated. Anyway, at least in the lower mass range, the impulse voltage including the stochastic potential is clearly quite suitable for the quadrupole ion trap with higher mass resolution. The fractional resolutions obtained are $(m/\Delta m)_{\eta=0} = 298$ and $(m/\Delta m)_{\eta=0.14} = 1113$; therefore, $(\Delta m)_{\eta=0.14} < (\Delta m)_{\eta=0}$ and this indicates that $\eta = 0.14$ when higher resolution in mass separation is involved.

Author's contributions

All authors read and approved the final manuscript.

Competing interests

The authors declare that they have no competing interests.

Acknowledgements

The authors thank the referees for valuable comments and suggestions which improved the presentation of this manuscript.

References

1. Blaum, K. *Phys. Rep*. **2006**, 425, 1.
2. Douglas, D. J.; Frank, A. J.; Mao, D. M. *Mass Spectrom. Rev*. **2005**, 24, 1.
3. Kingdon, K . H. *Phys. Rev.* **1923**, 21, 408.
4. Hu, Q. Z.; Noll, R. J.; Li, H. Y.; Makarov, A.; Hardman, M.; Cooks, R. G. *J. Mass Spectrom.* **2005**, 40, 430.
5. Seddighi Chaharborj, S.; Sadat Kiai, S. M. *J. Mass Spectrom.* **2010**, 45, 1111.
6. Paul, W.; Steinwedel, H. Z. Naturforsch. **1953**, 8, 448.
7. Kashanian, F.; Nouri, S.; Seddighi Chaharborj, S.; Mohd Rizam, A. B. *Int. J. Mass Spectrom.* **2011**, 303, 199.
8. Sadat Kiai, S.; M. Seddighi Chaharborj, S.; Abu Bakar, M. R.; Fudziah, I. *J. Anal. At. Spectrom.* **2011.** 26, 2247.
9. Seddighi Chaharborj, S.; Sadat Kiai, S. M.; Abu Bakar, M. R.; Ziaeian, I.; Fudziah, I. *Int. J. Mass Spectrom.* **2012**, 39, 63.
10. Itano, W. M.; Heinzen, D. J.; Bollinger, J. J.; Wineland, D. J. *Phys. Rev. A* **1990**, 41, 2295.
11. Rafac, R. J.; Young, B. C.; Beall, J. A.; Itano, W. M.; Wineland, D. J.; Berquist, J. C. *Phys. Rev. Lett.* **2000**, 85, 2462.
12. Kielpinski, D.; Meyer, V.; Rowe, M. A.; Sackett, C. A.;

Itano, W. M.; Monroe, C.; Wineland, D. J. *Science* **2001**, 291, 1013.
13. Beaty, E. C. *J. Appl. Phys.* **1987**, 61, 2118.
14. Seddighi Chaharborj, S.; Abu Bakar, M. R.; Fudziah, I. *Int. J. Mod. Phys.* **2012**, 9, 373.
15. Virginia, R. Y.; Thaleia, Z. *Insur. Math. Econ.* **2000**, 27. 1.
16. Denis, P. *IEEE Trans. Commun.* **2007**, 55, 1607.
17. Lorenzo, G. *IEEE Signal Proc. Let.* **2006**, 13, 608.
18. Seddighi Chaharborj, S.; Sadat Kiai, S. M.; Abu Bakar, M. R.; Ziaeian, I.; Fudziah, I. *Int. J. Mass Spectrom.* **2012**, 309, 63.
19. Seddighi Chaharborj, S.; Sadat Kiai, S. M. *J. Mass Spectrom.* **2010**, 45, 1111.
20. March, R. E. *J. Mass Spectrom.* **2000**, 200, 285.
21. Seddighi Chaharborj, S.; Phang, P. S.; Sadat Kiai, S. M.; Majid, Z. A.; Abu Bakar, M. R.; Fudziah, I. *Rapid Commun. Mass Spectrom.* **2012**, 26, 1481.